

The abundance of high-redshift objects as a probe of non-Gaussian initial conditions

Sabino Matarrese^{1,2}, Licia Verde³ and Raul Jimenez³

ABSTRACT

The observed abundance of high-redshift galaxies and clusters contains precious information about the properties of the initial perturbations. We present a method to compute analytically the number density of objects as a function of mass and redshift for a range of physically motivated non-Gaussian models. In these models the non-Gaussianity can be dialed from zero and is assumed to be small. We compute the probability density function for the *smoothed* dark matter density field and we extend the Press and Schechter approach to *mildly* non-Gaussian density fields. The abundance of high-redshift objects can be directly related to the non-Gaussianity parameter and thus to the physical processes that generated deviations from the Gaussian behaviour. Even a skewness parameter of order 0.1 implies a dramatic change in the predicted abundance of $z \gtrsim 1$ objects. Observations from NGST and X-ray satellites (XMM) can be used to accurately measure the amount of non-Gaussianity in the primordial density field.

Subject headings: Cosmology: theory—galaxies: clusters

1. Introduction

In the standard inflationary model for triggering structure formation in the Universe, there are precise predictions for the properties of the initial fluctuations: they are adiabatic and follow a nearly-Gaussian distribution, with deviations from Gaussianity which are calculable, small and generally dependent on the specific inflationary model (Falk et al. 1993; Gangui et al. 1994; Gangui 1994; Wang & Kamionkowski 1999; Gangui & Martin 1999). Because of the smallness of such deviations from the Gaussian behaviour, in most theoretical predictions one simply assumes that the primordial density field has *exactly* random phases. Consequently, intrinsic temperature fluctuations in the Cosmic Microwave Background (CMB) are commonly treated as being Gaussian and the same

¹Dipartimento di Fisica "Galileo Galilei", via Marzolo 8, I-35131 Padova, Italy. (matarrese@pd.infn.it)

²Max-Planck-Institut für Astrophysik, Karl-Schwarzschild-Strasse 1, D-85748 Garching, Germany. (sabino@mpa-garching.mpg.de)

³Institute for Astronomy, University of Edinburgh, Blackford Hill, Edinburgh EH9 3HJ, UK. (lv@roe.ac.uk, raul@roe.ac.uk)

assumption is made in most analyses of Large-Scale Structure (LSS) of the Universe. Besides this ‘standard’ nearly-Gaussian model for generating cosmological structures, based on the amplification of quantum fluctuations of the same scalar field which drives the inflationary dynamics, there exist alternative models for the origin of fluctuations which predict stronger deviations from the random-phase paradigm. Still within the context of inflation multiple scalar field models can give rise to non-Gaussian perturbations of either isocurvature or adiabatic type (Allen et al. 1987; Kofman & Pogosyan 1988; Salopek et al. 1989; Linde & Mukhanov 1997; Peebles 1999a,b; Salopek 1999). Alternatively, cosmological defect scenarios (e.g. Vilenkin 1985; Vachaspati 1986; Hill et al. 1989; Turok 1989; Albrecht & Stebbins 1992) generally predict non-Gaussian initial conditions.

The observed abundance of high-redshift cosmic structures contains important information about the properties of initial conditions on galaxy and clusters scales. CMB observations will put constraints on the nature of the initial conditions (e.g. Pen & Spergel 1995; Hu et al. 1997; Verde et al. 1999; Wang & Kamionkowski 1999; Wang et al. 1999), but will be severely affected by the presence of noise and foregrounds (e.g. Knox 1999; Tegmark 1998; Bouchet & Gispert 1999) and probe rather large scales.

The Gaussian assumption plays a central role in analytical predictions for the abundance and statistical properties of the first objects to collapse in the Universe. In this context, the formalism proposed by Press & Schechter (Press & Schechter 1974), with its later extensions and improvements (Peacock & Heavens 1990; Bond et al. 1991; Cole 1991; Lacey & Cole 1993) has become the ‘standard lore’ for predicting the number of collapsed dark matter halos as a function of redshift. However, even a small deviation from Gaussianity would have a deep impact on those statistics which probe the tails of the distribution. This is indeed the case for the abundance of high-redshift objects like galaxies at $z \gtrsim 5$ or clusters at $z \sim 1$ which correspond to high peaks, i.e. *rare events*, in the underlying dark matter density field. Therefore, even small deviations from Gaussianity might be potentially detectable by looking at the statistics of high-redshift systems.

The importance of using the mass-function as a tool to distinguish among different non-Gaussian statistics for the primordial density field, was first recognized by Lucchin & Matarrese (1988), Colafrancesco et al. (1989) and, more recently, by Chiu et al. (1998), followed by Robinson & Baker (1999), Robinson et al. (1999a,b), Koyama et al. (1999), Willick (1999), Avelino & Viana (1999). To make predictions on the number counts of high-redshift structures in the context of non-Gaussian initial conditions, a generalized version of the PS approach had to be introduced.

Such a generalization of the PS formalism has been tested successfully against N-body simulations (Robinson & Baker 1999), but, from a theoretical point of view, it suffers from the same problems of the original Press & Schechter (PS) formulation: it cannot properly account for the so called *cloud-in-cloud* problem, i.e. the constraint that bound systems of given mass should not be incorporated in larger mass condensations of the same catalog⁴. Even more important, most of

⁴The so called cloud-in-cloud problem arises only if one is interested in predicting the local density of maxima;

the PS generalizations to non-Gaussian models proposed in the literature do not properly take into account the dependence of the fluctuation field on the smoothing scale.

In this paper we obtain an analytic prediction for the number of dark matter halos as a function of redshift, within the hierarchical structure formation paradigm, following the PS formalism. The strength of our method is that we are able to properly take into account the smoothing-scale, or mass, dependence of the probability distribution function of the primordial density contrast. Obtaining analytical results in this context is extremely important. Direct simulations of non-Gaussian fields are generally plagued by the difficulty of properly accounting for the non-linear way in which resolution and finite box-size effects, present in any realization of the underlying Gaussian process, propagate into the statistical properties of the non-Gaussian field. Moreover, finite volume realizations of non-Gaussian fields might fail in producing fair samples of the assumed statistical distribution, i.e. ensemble and (finite-volume) spatial distributions might sensibly differ (e.g. Zel'dovich et al. 1987). This problem, of course, becomes exacerbated and hard to keep under control in so far as the tails of the distribution are concerned. Thus, in looking for the likelihood of rare events for a non-Gaussian density field, either exact or approximate analytical estimates should be considered as the primary tool.

When compared with N-body simulation results the striking feature of the standard PS algorithm is that it works extremely well in predicting properties of highly non-linear objects such as the DM haloes, even being based on linear theory and relatively simple assumptions. This agreement has been proven for Gaussian initial conditions, and one might wonder whether such a feature also extends to the non-Gaussian case, where additional non-linear couplings arise and non-linear gravitational corrections can be important at larger scales, unlike the Gaussian case. This extension of the PS prediction will be tested against N-body simulations in a subsequent paper. For the present application, however, the primordial non-Gaussianity is assumed to be small and we can safely assume that departures from the PS prediction are negligible.

The outline of the paper is as follows: in Section 2 we propose a parameterization of primordial non-Gaussianity that covers a wide range of physically motivated models whose non-Gaussianity can be dialed from zero (the Gaussian limit). We will then relate analytically the non-Gaussianity parameter to the number of high-redshift objects. This step involves the generalization of the PS formalism to non-Gaussian initial conditions, which in turn requires an expression for the probability density function of the non-Gaussian mass-density field as a function of the filtering radius. In Section 3, we calculate the probability density function for the density fluctuation field, smoothed on the mass scale typical of high-redshift objects. Since the non-Gaussianity is expected to be small, we can calculate the probability density function by expanding the ‘cumulant generator’ in powers of the non-Gaussianity parameter and keeping only linear order terms. In this context we are able to obtain an analytic expression for the probability density function of the smoothed

this feature is not a problem if one focuses the attention to percolation regions where the ratio of the local density ρ to the background density ρ_b is $\rho/\rho_b \sim 200$.

density field. We generalize the PS approach to non-Gaussian density fields in Section 4, where we give an analytical expression for the comoving mass-function of halos formed at a given redshift, also accounting for the cloud-in-cloud problem. Section 5 discusses the association between halos and high-redshift galaxies. The PS formalism predicts the number of dark matter halos, but the correspondence to the observed number of galaxies is not necessarily simple. Finally in Section 6 we summarize our main results and draw our conclusions.

2. Parameterization of primordial non-Gaussianity

Because of the infinite range of possible non-Gaussian models, we consider here two models with primordial non-Gaussianity, whose amplitude can be dialed from zero (the Gaussian limit). Following Verde et al. (1999) we consider models in which either the density contrast (**model A**) or the gravitational potential (**model B**) contains a part which is the square of a Gaussian random field. The physical motivation for this choice is that such a non-Gaussianity may arise in slow-roll and/or nonstandard (e.g. two-field) inflation models (Luo 1994; Falk et al. 1993; Gangui et al. 1994; Fan & Bardeen 1992); moreover both models may be considered as a Taylor expansion of more general non-Gaussian fields (e.g. Coles & Barrow 1987; Verde et al. 1999), and are thus fairly generic forms of *mild* non-Gaussianity.

We note here that, since in the PS framework the evolution of perturbations is considered to be linear, this parameterization of non-Gaussianity is effectively equivalent to non-linear biasing acting on a truly Gaussian underlying field. The effect of biasing is to alter the clustering properties of the galaxies with respect to the dark matter by relating galaxy formation efficiency to the environment. We do not intend to investigate the clustering properties of high-redshift objects, we will instead focus on the probability density function (PDF) of the linear density contrast as a tool to predict the abundance of dark matter halos as a function of mass and formation redshift.

2.1. Linear plus quadratic model for the density or the gravitational potential

As a first step, we want to obtain the PDF for a model where either the primordial over-density field $\delta \equiv \delta\rho/\rho$, or the initial peculiar gravitational potential Φ is represented by a zero-mean random field ψ , given by the following local transformation \mathcal{F} on an underlying Gaussian field ϕ :

$$\psi(\mathbf{x}) = \mathcal{F}[\phi] \equiv \alpha\phi(\mathbf{x}) + \epsilon(\phi^2(\mathbf{x}) - \langle\phi^2\rangle), \quad (1)$$

with α and ϵ free parameters of the model. The homogeneous and isotropic Gaussian process ϕ is assumed to have zero mean, $\langle\phi\rangle = 0$, and power-spectrum P_ϕ to be specified later. Note that in the limit $\alpha \rightarrow 0$, ψ is chi-squared distributed, while for $\epsilon \rightarrow 0$ one recovers the Gaussian case. As pointed out before, the model of eq. (1) can be thought as representing the first two terms of the Taylor expansion of more general non-Gaussian fields around the Gaussian limit. Cubic or higher

order powers of ϕ in such an expansion should be thought as being of order ϵ^2 or higher. We will come back to this point in Section 3.3. Since the overall normalization of ψ is fixed observationally (e.g. by measurements of the power-spectrum), effectively there is only one free parameter in the model. In what follows we will take either $\alpha = 1$ and ϵ as the non-Gaussianity parameter or $\alpha = 0$ and $\epsilon = 1$ to obtain the χ^2 model.

If there was no filtering to take into account or if the transformation (1) were true for a smoothed field, then the PDF for ψ could be simply obtained as follows

$$P(\psi) \equiv \langle \delta^D(\alpha\phi + \epsilon(\phi^2 - \langle \phi^2 \rangle) - \psi) \rangle \equiv \int d\phi P(\phi) \delta^D(\alpha\phi + \epsilon(\phi^2 - \langle \phi^2 \rangle) - \psi) \quad (2)$$

where $P(\phi)$ is a Gaussian PDF with zero mean and variance $\langle \phi^2 \rangle$ and δ^D is the Dirac delta function. The above equation can be also thought as resulting from applying the Chapman-Kolmogorov equation: $P(\psi) = \int d\phi W(\psi|\phi)P(\phi)$ where $W(\psi|\phi) = \delta^D(\psi - \mathcal{F}[\phi])$ is the transition probability from ϕ to ψ (e.g. Taylor & Watts 2000). The integral over ϕ can be performed by writing:

$$P(\psi) = \int d\phi P(\phi) \delta^D(\phi - \mathcal{F}^{-1}[\psi]) \frac{1}{d\mathcal{F}/d\phi}, \quad (3)$$

which gives:

$$P(\psi) = \{2\pi\langle \phi^2 \rangle [\alpha^2 + 4\epsilon(\epsilon\langle \phi^2 \rangle + \psi)]\}^{-1/2} [\mathcal{E}_-(\psi) - \mathcal{E}_+(\psi)], \quad (4)$$

with

$$\mathcal{E}_\pm(\psi) \equiv \exp \left\{ \frac{-1}{\epsilon^2\langle \phi^2 \rangle} \left[\alpha^2 + 2\epsilon(\epsilon\langle \phi^2 \rangle + \psi) \pm \alpha\sqrt{\alpha^2 + 4\epsilon(\epsilon\langle \phi^2 \rangle + \psi)} \right] \right\}. \quad (5)$$

However, in order to apply the PS formalism, we need to know the PDF for the linear mass-density field as a function of the smoothing radius R and redshift z . To take into account the different evolution of modes inside the horizon, we assume that the transfer function acts on our primordial non-Gaussian field $\psi(\mathbf{x})$, as a convolution. We can easily account for the smoothing operation, the effect of the transfer function and the linear growth of perturbations, by writing (e.g. Moscardini et al. 1991):

$$\delta_R(\mathbf{x}, z) = D(z)\delta_R(\mathbf{x}) = D(z) \int d^3y F_R(|\mathbf{x} - \mathbf{y}|) \psi(\mathbf{y}), \quad (6)$$

where $D(z)$ is the growing mode of linear perturbations, normalized to unity at $z = 0$, so that $\delta_R(\mathbf{x})$ represents the mass density fluctuation field linearly extrapolated to the present time. The isotropic function $F_R(|\mathbf{x}|)$ can be specified by its Fourier transform,

$$\tilde{F}_R(k) \equiv \int d^3y e^{-i\mathbf{k}\cdot\mathbf{y}} F(|\mathbf{y}|) = \tilde{W}_R(k) T(k) g(k), \quad (7)$$

where $\tilde{W}_R(k)$ is the Fourier transform of the assumed low-pass filter (e.g. a spherical top-hat filter), $T(k)$ is the transfer function (normalized to unity for $k \rightarrow 0$), that we will later assume to take the adiabatic CDM form as in (Bardeen et al. 1986), with the modifications of Sugiyama (1995).

The function $g(k)$ completes the specification of our model:

- **model A:** $g(k) = 1$, if we assume that our non-Gaussian model applies directly to the primordial density field.
- **model B:** $g(k) = -\frac{2}{3}(k/H_0)^2\Omega_{0m}^{-1}$, if the same assumption is made for the gravitational potential (its precise form comes from solving the cosmic Poisson equation); here Ω_{0m} denotes the present day density parameter of non-relativistic – baryonic plus dark – matter.

As widely discussed by Moscardini et al. (1991), the overall sign of the Gaussian to non-Gaussian mapping inherent in these models is a crucial parameter, which determines most of the non-linear dynamics. In our case, we are still free to choose the sign, through the actual choice of the free parameter ϵ . We finally get

$$\delta_R(\mathbf{x}) = \alpha\phi_R(\mathbf{x}) + \epsilon \int d^3y F_R(|\mathbf{x} - \mathbf{y}|)\phi^2(\mathbf{y}) - C, \quad (8)$$

where $\phi_R(\mathbf{x})$ is just the smoothed underlying Gaussian field i.e. the convolution of ϕ with F , and

$$C \equiv \epsilon\langle\phi^2\rangle \int d^3y F_R(|\mathbf{x} - \mathbf{y}|) \quad (9)$$

ensures that δ_R has zero expectation value.

3. PDF of the smoothed density fluctuations

In this section we derive an approximate analytic expression, valid for small values of the non-Gaussian parameter ϵ , for the PDF as a function of the smoothing radius (i.e. mass scale) and of the redshift of collapse. This is the key ingredient to develop the extension of the PS formalism to non-Gaussian fields. The reader mainly interested in the application of the PS approach to non-Gaussian density fields may omit reading this section at a first sitting.

Once the filtering process has been taken into account, the density fluctuation PDF can be obtained through a functional or *path-integral*⁵ (e.g. Ramond 1989)

$$\begin{aligned} P(\delta_R) &= \langle \delta^D \left(\alpha\phi_R(\mathbf{x}) + \epsilon \int d^3y F_R(|\mathbf{x} - \mathbf{y}|)\phi^2(\mathbf{y}) - C - \delta_R(\mathbf{x}) \right) \rangle \\ &= \int [\mathcal{D}\phi] \mathcal{P}[\phi] \int \frac{d\lambda}{2\pi} \exp \left[i\lambda \left(\alpha\phi_R(\mathbf{x}) + \epsilon \int d^3y F_R(|\mathbf{x} - \mathbf{y}|)\phi^2(\mathbf{y}) - C - \delta_R(\mathbf{x}) \right) \right], \end{aligned} \quad (10)$$

where, in the second line, we used the integral representation of the Dirac delta function. The functional integration is over ϕ configurations in real space weighted by the Gaussian probability

⁵The path-integral approach has been widely applied in the cosmological context and in particular to large-scale structure studies by e.g. Politzer & Wise (1984); Grinstein & Wise (1986); Matarrese, Lucchin & Bonometto (1986); Bertschinger (1987).

density functional

$$\mathcal{P}[\phi] = \exp \left\{ -\frac{1}{2} \int d^3 y \int d^3 z \phi(\mathbf{y}) \mathcal{K}(\mathbf{y}, \mathbf{z}) \phi(\mathbf{z}) \right\} / \int [\mathcal{D}\phi] \exp \left\{ -\frac{1}{2} \int d^3 y \int d^3 z \phi(\mathbf{y}) \mathcal{K}(\mathbf{y}, \mathbf{z}) \phi(\mathbf{z}) \right\} , \quad (11)$$

which has been consistently normalized to unit total probability, $\int [\mathcal{D}\phi] \mathcal{P}[\phi] = 1$.

Although the previous expressions for the PDF actually gives its form at redshift $z = 0$, one should keep in mind that the quantity $P(\delta_R) d\delta_R$ is redshift-independent, as long as linear evolution applies.

From now on we will use the following compact notation:

$$\int d^3 y \int d^3 z \phi(\mathbf{y}) \mathcal{K}(\mathbf{y}, \mathbf{z}) \phi(\mathbf{z}) \equiv (\phi, \mathcal{K}, \phi) \quad (12)$$

The symmetric kernel \mathcal{K} is defined as the functional inverse of the two-point correlation function $\xi_\phi(\mathbf{y}, \mathbf{w}) = \xi_\phi(|\mathbf{y} - \mathbf{w}|)$ of the field ϕ , namely,

$$\int d^3 y \mathcal{K}(\mathbf{z}, \mathbf{y}) \xi_\phi(\mathbf{y}, \mathbf{w}) = \delta^D(\mathbf{z} - \mathbf{w}) . \quad (13)$$

By exploiting the fact that

$$\int d^3 y F_R(|\mathbf{x} - \mathbf{y}|) \phi^2(\mathbf{y}) = \int d^3 y \int d^3 z \phi(\mathbf{y}) F_R(|\mathbf{x} - \mathbf{y}|) \delta^D(\mathbf{y} - \mathbf{z}) \phi(\mathbf{z}) \equiv (\phi, F_R \delta^D, \phi), \quad (14)$$

equation (11) becomes:

$$P(\delta_R) = \frac{\int \frac{d\lambda}{2\pi} e^{-i\lambda\delta_R - i\lambda C} \int [\mathcal{D}\phi] \exp \left\{ -\frac{1}{2} (\phi, \mathcal{K}, \phi) + i\lambda \epsilon (\phi, F_R \delta^D, \phi) + i(\mathcal{J}_\lambda, \phi) \right\}}{\int [\mathcal{D}\phi] e^{-\frac{1}{2} (\phi, \mathcal{K}, \phi)}} , \quad (15)$$

where we have defined the *source* functional

$$\mathcal{J}_\lambda(\mathbf{y}) \equiv \lambda \alpha F_R(|\mathbf{x} - \mathbf{y}|) \quad (16)$$

and introduced the notation

$$(\mathcal{J}_\lambda, \phi) \equiv \int d^3 y \mathcal{J}_\lambda(\mathbf{y}) \phi(\mathbf{y}) . \quad (17)$$

The above functional integration can be performed analytically, by applying the so-called path-integral technique for *composite operators* (Cornwall et al. 1974; Hawking & Moss 1983). Let us briefly sketch the main steps of the procedure.

We start by defining a new kernel:

$$\mathcal{K}'_\lambda(\mathbf{z}, \mathbf{y}) \equiv \mathcal{K}(\mathbf{z}, \mathbf{y}) - i2\lambda\epsilon F_R(|\mathbf{y} - \mathbf{x}|) \delta^D(\mathbf{z} - \mathbf{y}) , \quad (18)$$

which allows to write

$$P(\delta_R) = \int \frac{d\lambda}{2\pi} e^{-i\lambda\delta_R - i\lambda C} \int [\mathcal{D}\phi] e^{-\frac{1}{2}(\phi, \mathcal{K}'_\lambda, \phi) + i(\mathcal{J}_\lambda, \phi)}. \quad (19)$$

We then make the change of variable (under which the path-integral is left unchanged)

$$\phi(\mathbf{z}) \rightarrow \phi(\mathbf{z}) - i \int d^3y [\mathcal{K}'_\lambda]^{-1}(\mathbf{z}, \mathbf{y}) \mathcal{J}_\lambda(\mathbf{y}) \quad (20)$$

where $[\mathcal{K}'_\lambda]^{-1}$ satisfies the integral equation

$$\int d^3y \mathcal{K}'(\mathbf{z}, \mathbf{y}) [\mathcal{K}'_\lambda]^{-1}(\mathbf{y}, \mathbf{w}) = \delta^D(\mathbf{z} - \mathbf{w}). \quad (21)$$

We then easily get:

$$P(\delta_R) = \int \frac{d\lambda}{2\pi} e^{-i\lambda\delta_R - i\lambda C - \frac{1}{2}(\mathcal{J}_\lambda, [\mathcal{K}'_\lambda]^{-1}, \mathcal{J}_\lambda)} \{ \text{Det}[\mathcal{K}'_\lambda] / \text{Det}[\mathcal{K}] \}^{-1/2}, \quad (22)$$

having used the standard notation for functional determinants:

$$\{ \text{Det}[\mathcal{K}'_\lambda] / \text{Det}[\mathcal{K}] \}^{-1/2} \equiv \frac{\int [\mathcal{D}\phi] \exp[-\frac{1}{2}(\phi, \mathcal{K}'_\lambda, \phi)]}{\int [\mathcal{D}\phi] \exp[-\frac{1}{2}(\phi, \mathcal{K}, \phi)]} = \exp \left\{ -\frac{1}{2} \text{Tr} \ln [\mathbf{1} - i2\lambda\epsilon(F_R\delta^D, \mathcal{K}^{-1})] \right\}. \quad (23)$$

The reader unfamiliar with the functional notation can understand the last result as a generalization of the identity $\ln[\det \mathbf{M}] = \text{Tr}[\ln \mathbf{M}]$, which applies to any symmetric matrix \mathbf{M} . Here $\mathbf{1}$ denotes the functional unit matrix, i.e. the Dirac delta function; the logarithm of a functional is defined as its series expansion and

$$(F_R\delta^D, \mathcal{K}^{-1}) \equiv \int d^3w F_R(|\mathbf{w} - \mathbf{x}|) \delta^D(\mathbf{y} - \mathbf{w}) \mathcal{K}^{-1}(\mathbf{w} - \mathbf{z}) = F_R(|\mathbf{y} - \mathbf{x}|) \xi_\phi(\mathbf{y} - \mathbf{z}). \quad (24)$$

Finally, the trace (Tr) of a functional $G(\mathbf{y}, \mathbf{z})$ is defined as $\int d^3y \int d^3z \delta^D(\mathbf{y} - \mathbf{z}) G(\mathbf{y}, \mathbf{z})$.

Therefore, equation (23) becomes:

$$\{ \text{Det}[\mathcal{K}'_\lambda] / \text{Det}[\mathcal{K}] \}^{-1/2} = \exp \left\{ -\frac{1}{2} \int d^3y \int d^3z \delta^D(\mathbf{y} - \mathbf{z}) \ln [\delta^D(\mathbf{y} - \mathbf{z}) - i2\lambda\epsilon F_R(|\mathbf{y} - \mathbf{x}|) \xi_\phi(\mathbf{y} - \mathbf{z})] \right\} \quad (25)$$

The PDF for the linearly evolved, smoothed density field takes the exact form:

$$P(\delta_R) d\delta_R = \int \frac{d\lambda}{2\pi} e^{-i\lambda\delta_R + \mathcal{W}(\lambda)} d\delta_R, \quad (26)$$

where $\mathcal{W}(\lambda)$ is called the *cumulant generator*, as its series expansion around $\lambda = 0$ defines the cumulants (or irreducible moments) of $\delta_R(\mathbf{x})$. Its exact form is:

$$\begin{aligned} \mathcal{W}(\lambda) &= -i\lambda C - \frac{1}{2} \int d^3y \int d^3z \left\{ \lambda^2 \alpha^2 F_R(|\mathbf{y}|) [\mathcal{K}'_\lambda]^{-1}(\mathbf{y}, \mathbf{z}) F_R(|\mathbf{z}|) \right. \\ &\quad \left. + \delta^D(\mathbf{y} - \mathbf{z}) \ln [\delta^D(\mathbf{y} - \mathbf{z}) - i2\lambda\epsilon F_R(|\mathbf{y}|) \xi_\phi(\mathbf{y} - \mathbf{z})] \right\}. \end{aligned} \quad (27)$$

where the λ subscript indicates where the λ dependence is hidden. Note that the \mathbf{x} dependence has been eliminated by a mere translation of the origin. Equation (27) contains also the exact form for the generating function for the particular case where the original non-Gaussian field ψ is chi-squared distributed: this is simply obtained by setting $\alpha = 0$ in the previous expression. Note also that the first-order term in the expansion of the logarithm precisely cancels the $-i\lambda C$ term, so that the condition $\langle \delta_R \rangle = 0$ is identically satisfied.

3.1. Kernel inversion

In order to solve the remaining integrals we need to find an expression for the functional $[\mathcal{K}'_\lambda]^{-1}$. Let us start by finding an expression for the kernel \mathcal{K} , given that its inverse is just the auto-correlation function of the Gaussian field ϕ , namely,

$$\int d^3y \mathcal{K}(\mathbf{w} - \mathbf{y}) \xi_\phi(|\mathbf{y} - \mathbf{z}|) = \delta^D(\mathbf{w} - \mathbf{z}) . \quad (28)$$

Fourier transforming both sides of eq. (28) we easily find (Politzer & Wise 1984; Bertschinger 1987)

$$\tilde{\mathcal{K}}(k) = 1/P_\phi(k) \quad (29)$$

where $P_\phi(k)$ is the power-spectrum of the underlying Gaussian field ϕ . Therefore $\mathcal{K}(\mathbf{w}, \mathbf{y}) \equiv \mathcal{K}(|\mathbf{w} - \mathbf{y}|) \equiv \mathcal{K}(r)$ reads

$$\mathcal{K}(r) = \frac{1}{(2\pi)^3} \int d^3k \exp(i\mathbf{k} \cdot \mathbf{r}) \frac{1}{P_\phi(k)} = \frac{1}{2\pi^2} \int_0^\infty dk k^2 j_0(kr) \frac{1}{P_\phi(k)} . \quad (30)$$

To find an expression for $[\mathcal{K}'_\lambda]^{-1}$ one would like to proceed in an analogous way. However, owing to the absence of translational invariance of \mathcal{K}' , going to momentum space does not help. The technique we are then going to use is to expand $[\mathcal{K}'_\lambda]^{-1}$ in powers of the non-Gaussianity parameter ϵ , as follows:

$$[\mathcal{K}'_\lambda]^{-1}(\mathbf{y}, \mathbf{z}) = \sum_{n=0}^{\infty} (2i\epsilon\lambda)^n \mathcal{R}^{(n)}(\mathbf{y}, \mathbf{z}) \quad (31)$$

where the coefficients $\mathcal{R}^{(n)}$ are obtained recursively from

$$\mathcal{R}^{(n)}(\mathbf{y}, \mathbf{z}) = \int d^3w \xi_\phi(|\mathbf{y} - \mathbf{w}|) F_R(|\mathbf{w}|) \mathcal{R}^{(n-1)}(\mathbf{w}, \mathbf{z}) \quad (n > 0) , \quad (32)$$

with $\mathcal{R}^{(0)}(\mathbf{y}, \mathbf{z}) = \xi_\phi(|\mathbf{y} - \mathbf{z}|)$. Similarly, in Fourier space we have

$$\tilde{\mathcal{R}}^{(n)}(\mathbf{k}, \mathbf{k}') = P_\phi(k) \int \frac{d^3q}{(2\pi)^3} \tilde{F}_R(q) \tilde{\mathcal{R}}^{(n-1)}(\mathbf{q} + \mathbf{k}, \mathbf{k}') , \quad (33)$$

with $\tilde{\mathcal{R}}^{(0)}(\mathbf{k}, \mathbf{k}') = (2\pi)^3 P_\phi(k) \delta^D(\mathbf{k} + \mathbf{k}')$.

From equation (33) we find:

$$\tilde{\mathcal{R}}^{(1)}(\mathbf{k}, \mathbf{k}') = P_\phi(k)P_\phi(k')\tilde{F}_R(|\mathbf{k} + \mathbf{k}'|) \quad (34)$$

and, for $n \geq 2$,

$$\begin{aligned} \tilde{\mathcal{R}}^{(n)}(\mathbf{k}, \mathbf{k}') &= P_\phi(k)P_\phi(k') \int \frac{d^3q_1}{(2\pi)^3} \cdots \int \frac{d^3q_{n-1}}{(2\pi)^3} \tilde{F}_R(q_1) \cdots \tilde{F}_R(q_{n-1}) \\ &\times \tilde{F}_R(|\mathbf{q}_1 + \cdots + \mathbf{q}_{n-1} + \mathbf{k} + \mathbf{k}'|) P_\phi(|\mathbf{q}_1 + \mathbf{k}|) \cdots P_\phi(|\mathbf{q}_{n-1} + \mathbf{k}|) . \end{aligned} \quad (35)$$

Note that, while in principle the expressions for \mathcal{K}' , $\mathcal{R}^{(n)}$ and $\tilde{\mathcal{R}}^{(n)}$ should be symmetrized, for the purpose of calculating the PDF or the cumulants, this operation is not needed.

3.2. Cumulant generator

At this point we are ready to provide an expression for the cumulant generator, by first expanding it in powers of λ . We have:

$$\mathcal{W}(\lambda) \equiv \sum_{n=2}^{\infty} \frac{(i\lambda)^n}{n!} \mu_{n,R} , \quad (36)$$

where $\mu_{n,R}$ denotes the cumulant of order n of the smoothed density contrast δ_R .

The variance, the skewness and the kurtosis of the smoothed non-Gaussian density field are, respectively ⁶,

$$\begin{aligned} \mu_{2,R} &\equiv \sigma_R^2 \equiv \langle \delta_R^2 \rangle = \frac{\alpha^2}{2\pi^2} \int_0^\infty dk k^2 \tilde{F}_R^2(k) P_\phi(k) \\ &+ \frac{\epsilon^2}{2\pi^4} \int_0^\infty dk k^2 P_\phi(k) \int_0^\infty dk' k'^2 P_\phi(k') \int_0^1 d\mu \tilde{F}_R^2(\sqrt{k^2 + k'^2 + 2kk'\mu}) , \end{aligned} \quad (37)$$

$$\begin{aligned} \mu_{3,R} &\equiv \langle \delta_R^3 \rangle = \frac{3\epsilon\alpha^2}{2\pi^4} \int_0^\infty dk k^2 \tilde{F}_R(k) P_\phi(k) \int_0^\infty dk' k'^2 \tilde{F}_R(k') P_\phi(k') \int_0^1 d\mu \tilde{F}_R(\sqrt{k^2 + k'^2 + 2kk'\mu}) \\ &+ 8\epsilon^3 \int \frac{d^3k_1}{(2\pi)^3} \int \frac{d^3k_2}{(2\pi)^3} \int \frac{d^3k_3}{(2\pi)^3} P_\phi(k_1) P_\phi(k_2) P_\phi(k_3) \tilde{F}_R(|\mathbf{k}_1 - \mathbf{k}_2|) \tilde{F}_R(|\mathbf{k}_2 - \mathbf{k}_3|) \tilde{F}_R(|\mathbf{k}_3 - \mathbf{k}_1|) . \end{aligned} \quad (38)$$

⁶The integral over k in the sub-leading term of the variance can diverge for certain choices of the power-spectrum of the underlying Gaussian field and transfer function. In these cases one should bear in mind that any physical process originating the underlying field will necessarily provide the ϕ power-spectrum with both infrared and ultraviolet cutoffs (the present-day horizon and the reheating scale, respectively, in the case of inflation-generated perturbations). In case this contribution dominates over the leading-order contribution even for $\epsilon \ll 1$ one can postulate the existence of a term proportional to ϵ^2 in eq. (1) that will cancel out the sub-leading term in the variance. Alternatively eq. (1) and eq. (37) can be renormalized by choosing α and A_ϕ such that $\mu_{2,R} \simeq \mu_{2,R}^{(1)}$ when $\epsilon \ll 1$. Our calculations still apply in this case provided one interprets ϵ as ϵ/α^2 .

and

$$\begin{aligned}
\mu_{4,R} &\equiv \langle \delta_R^4 \rangle - 3\langle \delta_R^2 \rangle^2 \\
&= 48\epsilon^2 \alpha^2 \int \frac{d^3 k_1}{(2\pi)^3} \int \frac{d^3 k_2}{(2\pi)^3} \int \frac{d^3 k_3}{(2\pi)^3} P_\phi(k_1) P_\phi(k_2) P_\phi(|\mathbf{k}_3 + \mathbf{k}_1|) \tilde{F}_R(k_1) \tilde{F}_R(k_2) \tilde{F}_R(k_3) \\
&\times \tilde{F}_R(|\mathbf{k}_1 + \mathbf{k}_2 + \mathbf{k}_3|) + 96\epsilon^4 \int \frac{d^3 k_1}{(2\pi)^3} \int \frac{d^3 k_2}{(2\pi)^3} \int \frac{d^3 k_3}{(2\pi)^3} \int \frac{d^3 k_4}{(2\pi)^3} P_\phi(k_1) P_\phi(k_2) P_\phi(k_3) P_\phi(k_4) \\
&\times \tilde{F}_R(|\mathbf{k}_1 - \mathbf{k}_2|) \tilde{F}_R(|\mathbf{k}_2 - \mathbf{k}_3|) \tilde{F}_R(|\mathbf{k}_3 - \mathbf{k}_4|) \tilde{F}_R(|\mathbf{k}_4 - \mathbf{k}_1|) .
\end{aligned} \tag{39}$$

More in general, the cumulants are made of two contributions: a leading term of order ϵ^{n-2} plus a subleading term of order ϵ^n ,

$$\mu_{n,R} \equiv \epsilon^{n-2} \mu_{n,R}^{(1)} + \epsilon^n \mu_{n,R}^{(2)}, \tag{40}$$

where

$$\mu_{n,R}^{(1)} = 2^{n-3} n! \alpha^2 \int \frac{d^3 k}{(2\pi)^3} \int \frac{d^3 k'}{(2\pi)^3} \tilde{F}_R(k_1) \tilde{F}_R(k_2) \tilde{\mathcal{R}}^{(n-2)}(\mathbf{k}, \mathbf{k}') \tag{41}$$

and

$$\mu_{n,R}^{(2)} = 2^{n-1} (n-1)! \int \frac{d^3 k_1}{(2\pi)^3} \cdots \int \frac{d^3 k_n}{(2\pi)^3} P_\phi(k_1) \cdots P_\phi(k_n) \tilde{F}_R(|\mathbf{k}_1 - \mathbf{k}_2|) \cdots \tilde{F}_R(|\mathbf{k}_{n-1} - \mathbf{k}_n|) \tilde{F}_R(|\mathbf{k}_n - \mathbf{k}_1|) . \tag{42}$$

Note that, as anticipated, the sign of the parameter ϵ , for a given model, fully determines the sign of the skewness as well as of all the other odd-order cumulants.

The cumulants for the filtered chi-squared model are immediately recovered by taking $\alpha = 0$ and $\epsilon = 1$ in the previous expressions, so that $\mu_{n,R} = \mu_{n,R}^{(2)}$. It is worth noticing that eq. (42) supplies *all* the cumulants of a chi-squared field smoothed on scale R . This is an interesting result for models such as that recently proposed by Peebles (1999a,b), where non-Gaussian isocurvature fluctuations are obtained with a chi-squared distributed density field.

3.2.1. Linear order in ϵ

To first order, the skewness depends linearly on ϵ , therefore let us define

$$S_{3,R} \equiv \epsilon S_{3,R}^{(1)} = \epsilon \mu_{3,R}^{(1)} / (\mu_{2,R}^{(1)})^2, \tag{43}$$

where

$$\mu_{2,R}^{(1)} = \frac{\alpha^2}{2\pi^2} \int_0^\infty dk k^2 \tilde{F}_R^2(k) P_\phi(k) \tag{44}$$

and

$$\mu_{3,R}^{(1)} = \langle \delta_R^3 \rangle = \frac{3\alpha^2}{2\pi^4} \int_0^\infty dk k^2 \tilde{F}_R(k) P_\phi(k) \int_0^\infty dk' k'^2 \tilde{F}_R(k') P_\phi(k') \int_0^1 d\mu \tilde{F}_R(\sqrt{k^2 + k'^2 + 2kk'\mu}) \quad (45)$$

To this order in ϵ there is no contribution from higher order moments. On very large scales, where the transfer function becomes unity, and for a power-law ϕ power-spectrum ($P_\phi = A_\phi k^n$ or $P_\phi = A_\phi k^{n-3}$ for model A or B, respectively), this leading-order skewness parameter $S_{3,R}$ becomes scale-independent, thus mimicking the behaviour induced by the gravitational instability (Peebles 1980). For model A the variance, the skewness $\mu_{3,R}^{(1)}$ and skewness parameter $S_{3,R}$ are plotted vs. the radius R and the mass M in solar masses, $M \propto R^3$, in Figure 1 with the following assumptions: $\alpha = 1$, top-hat filter in real space, transfer function as in (Sugiyama 1995), with baryonic matter density parameter $\Omega_{0b} = 0.015h^{-2}$, $h = 0.65$, $\Omega_{0m} = 0.3$, and scale-invariant primordial power-spectrum $P_\phi \propto k$, normalized so that the present day r.m.s. fluctuation on a sphere of $8 h^{-1}$ Mpc is $\sigma_8 = 0.99$ (Viana & Liddle 1998), which simultaneously allows to best fit the local cluster abundance and the *COBE* data (e.g. Tegmark 1996). In what follows we will always assume that the approximation $\sigma_R^2 \equiv \mu_{2,R}^{(1)}$ applies on all considered scales. As detailed below, at $z = 0$, for $\epsilon \leq 0.01$ in model A we will recover the standard PS mass-function on clusters scales, so that the relation between the observed abundance of clusters and the value of σ_8 keeps unchanged, in spite of our non-Gaussian assumption.

To deal with model B we take $P_\phi \propto k^{-3}$ and, as above, we normalize the mass-density variance as in model A, with the same choice of cosmological parameters and transfer function. The variance, the skewness $\mu_{3,R}^{(1)}$ and skewness parameter $S_{3,R}^{(1)}$ are plotted vs. the radius R and the mass M in solar masses, $M \propto R^3$, in Figure 2 with the same assumptions as for model A in Figure 1. The variance for model B to linear order in ϵ is identical to the variance for model A, but the skewness and skewness parameter are different: in particular notice that $S_{3,R}^{(1)}$ for model B has the opposite sign of ϵ and, for a given value of ϵ , its amplitude is many orders of magnitude smaller than for model A. It is important to realize, that both signs for ϵ are generally allowed. In the inflationary case, both the sign and the magnitude of ϵ are related to the inflationary slow-roll parameters ϵ_{infl} and η_{infl} (Gangui et al. 1994; Gangui 1994; Wang & Kamionkowski 1999; Gangui & Martin 1999). In this model, the PS mass-function at $z = 0$ is practically recovered on all scales, for all $|\epsilon| \lesssim 200$.

3.2.2. Quadratic order in ϵ

For small deviations from Gaussianity, a first-order expansion in ϵ is a valid approximation. We give here the expressions for the relevant quantities also to second order, but in any application we will neglect second or higher-order corrections.

When expanding the cumulant generator to second order in ϵ we obtain that the variance has a contribution $\propto \epsilon^2$ as in eq. (37), the skewness remains the same as to first-order in ϵ , the next to

leading term being $\propto \epsilon^3$, but there is a non-vanishing contribution to the kurtosis $\propto \epsilon^2$, namely

$$\begin{aligned} \mu_{4,R} &= \epsilon^2 \mu_{4,R}^{(1)} = 48\epsilon^2 \alpha^2 \int \frac{d^3 k_1}{(2\pi)^3} \int \frac{d^3 k_2}{(2\pi)^3} \int \frac{d^3 k_3}{(2\pi)^3} P_\phi(k_1) P_\phi(k_2) P_\phi(|\mathbf{k}_3 + \mathbf{k}_1|) \\ &\times \tilde{F}_R(k_1) \tilde{F}_R(k_2) \tilde{F}_R(k_3) \tilde{F}_R(|\mathbf{k}_1 + \mathbf{k}_2 + \mathbf{k}_3|) \end{aligned} \quad (46)$$

For both models, the leading-order kurtosis parameter $S_{4,R} = \epsilon^2 \mu_{4,R}^{(1)} / (\mu_{2,R}^{(1)})^3$ becomes scale-independent if the power-spectrum is a power-law; therefore on large scales, where the transfer function is unity, $S_{4,R}$ becomes scale-independent.

3.3. Higher order non-Gaussian contributions

What happens to our results if we allow for higher order terms in the original definition of our primordial non-Gaussian field ψ ? Let us modify, for instance, our definition by adding a cubic term, as follows,

$$\psi(\mathbf{x}) = \alpha\phi(\mathbf{x}) + \epsilon(\phi^2(\mathbf{x}) - \langle \phi^2 \rangle) + \epsilon^2 \beta \phi^3(\mathbf{x}) , \quad (47)$$

where β is a new independent parameter, which we assume to be of order unity. Such a cubic term might be easily accounted for in the functional integral approach, by using the so-called ‘integration by parts’ relation (e.g. Ramond 1989). For the purpose of the present paper, however, we can account for such a cubic term through the modifications it induces in the lowest-order cumulants. The sub-leading term of the variance would in fact be modified by the addition of

$$\epsilon^2 \Delta \mu_{2,R}^{(2)} = 6\epsilon^2 \frac{\beta}{\alpha} \langle \phi^2 \rangle \mu_{2,R}^{(1)} , \quad (48)$$

which therefore appears as a ‘renormalization’ of the leading-order variance. The sub-leading skewness would also get an extra contribution of the same order ϵ^3 , which we will not write here. The kurtosis, instead, would be modified already to leading order, gaining the extra piece

$$\epsilon^2 \Delta \mu_{4,R}^{(1)} = \frac{1}{2} \epsilon^2 \alpha \beta \mu_{4,R}^{(1)} , \quad (49)$$

which still has the nice feature of appearing as a renormalization of the previously calculated leading-order kurtosis.

At this point we can derive a general ⁷ and self-consistent approximation to the cumulant generator (and hence for both the differential and cumulative probability) up to order ϵ^2 :

$$\mathcal{W}(\lambda) = -\frac{\lambda^2}{2} \mu_{2,R}^{(1)} - \epsilon \frac{i\lambda^3}{6} \mu_{3,R}^{(1)} + \epsilon^2 \left[-\frac{\lambda^2}{2} (\mu_{2,R}^{(2)} + 6\frac{\beta}{\alpha} \langle \phi^2 \rangle \mu_{2,R}^{(1)}) + \frac{\lambda^4}{24} \left(1 + \frac{1}{2} \alpha \beta \right) \mu_{4,R}^{(1)} \right] . \quad (50)$$

⁷The key assumption that allowed us to obtain such a general treatment of a mildly non-Gaussian field is that it can be expanded as a local functional of an underlying Gaussian field. On the other hand, any form of non-locality such that it can be expressed as a convolution in real space can also be handled in a similar way, by suitably modifying our definition of the function $F_R(\mathbf{x})$.

This is the explicit expression for $\mathcal{W}(\lambda)$; no further terms could appear from higher-order non-Gaussianity to this order in ϵ . Substituting this expansion in eq. (26) one gets an approximate expression for the PDF as an integral over λ , which is valid for suitably small values of the non-Gaussian parameter ϵ .

For the rest of our calculations, however, we will assume that departures from Gaussianity are small and therefore we will retain only linear-order terms.

4. Press-Schechter approach to non-Gaussian density fields

To obtain the abundance of dark matter halos as a function of filtering radius R (or mass $M \propto R^3$) and redshift of collapse z_c , one should first obtain the conditional probability that the density contrast equals the threshold for collapse δ_c , when filtered on scale R , provided it is below it on any larger scale R' . In the Gaussian case, and for sharp-k-space filter, this problem has been solved by a number of authors (Peacock & Heavens 1990; Cole 1991; Bond et al. 1991) by rephrasing it in terms of the problem of barrier first-crossing by a Markovian random walk. In the non-Gaussian case and/or for other types of filters, different techniques might also be useful. In particular, an alternative formulation, originally proposed by Jedamzik (1995) and successively implemented by Yano, Nagashima & Gouda (1996), Nagashima & Gouda (1997) and Lee & Shandarin (1998), allows to reduce the problem to the solution of the integral equation,

$$P(> \delta_c | z_c, M) = \frac{1}{\bar{\rho}_{0m}} \int_0^\infty dM' P(M|M') M' n(M', z_c), \quad (51)$$

where $\bar{\rho}_{0m}$ is the present-day mean density of non-relativistic matter, $P(> \delta_c | z_c, M)$ is the probability that δ_M lies above the threshold δ_c (i.e. the fraction of volume where this happens) at a given redshift z_c and $n(M, z_c)$ is the required comoving mass-function for halos of mass between M and $M + dM$ which formed at z_c . The function $P(M|M')$ denotes the conditional probability of finding a region with mass M overdense by δ_c or more, given that it is included in an *isolated* region of mass M' ($> M$).

Let us start by first finding an expression for the L.H.S. of this equation, i.e. for the level-crossing probability $P(> \delta_c | z_c, M)$.

In looking at this problem, it is convenient to think of the density fluctuation as being time-independent while giving a redshift dependence to the collapse threshold $\delta_c(z_c) \equiv \Delta_c(z_c)/D(z_c | \Omega_{0m}, \Omega_{0\Lambda})$; Δ_c is the linear extrapolation of the over-density for spherical collapse: it is 1.686 in the Einstein-de Sitter case, while it slightly depends on redshift (see Figure 3) for more general cosmologies (e.g. Kitayama & Suto 1996); $\Omega_{0\Lambda}$ denotes the closure density of vacuum energy today. Here $D(z | \Omega_{0m}, \Omega_{0\Lambda})$ denotes the general expression for the linear growth factor, which depends on the background cosmology: the redshift dependence of $D(z_c | \Omega_{0m}, \Omega_{0\Lambda})^{-1}$ is shown in Figure 3 for three different cosmological models.

Using the spherical isothermal collapse model (Gunn & Gott 1972), it is possible to relate the mass M of a dark halo to the Lagrangian (pre-collapse) comoving length R (the sphere of radius R will give rise to an object that contains the mass M within the virialization radius) (e.g. White, Efstathiou & Frenk 1993),

$$R = \frac{2^{1/2}[V_c/100\text{kms}^{-1}]}{\Omega_{0m}^{1/2}(1+z_c)^{1/2}f_c^{1/6}} \quad (52)$$

where R is in units of Mpc h^{-1} . Here V_c is the circular velocity required for centrifugal support in the potential of the halo, given by $M = V_c^3/(10GH(z_c))$, where H denotes the Hubble constant, (e.g. Heavens & Jimenez 1999), and f_c is the density contrast at virialization of the newly-collapsed object relative to the background. This is adequately approximated by $f_c = 178/\Omega_m^{0.6}(z_c)$ (e.g. Eke, Cole & Frenk 1996).

In Figure 3 the dependence of (52) on the cosmology and the redshift of collapse is shown. It is clear that this dependence is very weak and can be ignored for our purposes. For a chosen power-spectrum shape and normalization, the dependence on the cosmological model of the PDF and the level excursion probability is therefore confined in $\delta_c(z_c)$. In other words, changing the cosmology is essentially equivalent to changing z_c according to the right panel of Figure 3.

Following the PS formalism, we can write

$$P(> \delta_c|z_c, R) = \int_{\delta_c(z_c)}^{\infty} d\delta_R P(\delta_R) = \int_{\delta_c(z_c)}^{\infty} d\delta_R \int_{-\infty}^{\infty} \frac{d\lambda}{2\pi} e^{-i\lambda\delta_R + \mathcal{W}(\lambda)}, \quad (53)$$

which, exchanging the order of integrations and integrating over δ_R , yields the exact and general expression

$$P(> \delta_c|z_c, R) = \frac{1}{2\pi i} \int_{-\infty}^{\infty} \frac{d\lambda}{\lambda} \exp[-i\lambda\delta_c(z_c) + \mathcal{W}(\lambda)] + \frac{1}{2}. \quad (54)$$

This is the exact expression for the probability that at redshift z_c , the fluctuation on scale R exceeds some critical value δ_c . From this equation it is possible to obtain an approximate expression for the cumulative probability $P(> \delta_c|z_c, R)$ by expanding $\mathcal{W}(\lambda)$ of eq. (27) to a given order in ϵ . On the other hand, from knowledge of the cumulants of the cosmological density field smoothed on scale R , up to some order, it is possible to obtain an approximate expression for the level excursion probability $P(> \delta|R)$.

The integral (54) can be solved analytically by using the *saddle-point* technique as in (Fry 1986) and (Lucchin & Matarrese 1988). We first perform a *Wick rotation*, $\lambda \rightarrow i\lambda$, in the complex λ plane, to get rid of the oscillatory behaviour of the integrand. This gives

$$P(> \delta_c|z_c, R) = \frac{1}{2\pi i} \int_{-i\infty}^{i\infty} \frac{d\lambda}{\lambda} \exp[-\lambda\delta_c(z_c) + \mathcal{M}(\lambda)] + \frac{1}{2}, \quad (55)$$

with $\mathcal{M}(\lambda) \equiv \mathcal{W}(-i\lambda)$. Next, let us introduce the *effective action* $G(\delta_{\text{eff}})$, defined as the Legendre transform of \mathcal{M} , namely $G(\delta_{\text{eff}}) = \lambda\delta_{\text{eff}} - \mathcal{M}(\lambda)$, with $\delta_{\text{eff}} = d\mathcal{M}/d\lambda$. From the definition of \mathcal{M}

one has

$$P(> \delta_c | z_c, R) = \frac{1}{2\pi i} \int_{G'=-i\infty}^{G'=i\infty} d\delta_{\text{eff}} \frac{G''(\delta_{\text{eff}})}{G'(\delta_{\text{eff}})} \exp [(\delta_{\text{eff}} - \delta_c(z_c)) G'(\delta_{\text{eff}}) - G(\delta_{\text{eff}})] + \frac{1}{2}. \quad (56)$$

For large thresholds, $\delta_c(z_c) \gg 1$, the above integral is dominated by stationary points of the exponential. These occur at $G''(\delta_{\text{eff}})(\delta_c(z_c) - \delta_{\text{eff}}) = 0$, i.e. at $\delta_{\text{eff}} = \delta_c(z_c)$, since $G''(\delta_{\text{eff}}) = (d^2 \mathcal{M}/d\lambda^2)^{-1} > 0$ [as \mathcal{M} must be a convex function of its argument (e.g. Fry 1985)]. A saddle-point evaluation of this integral then gives (Lucchin & Matarrese 1988)

$$P(> \delta_c | z_c, R) \approx \frac{1}{\sqrt{2\pi}} \frac{(G'')^{1/2}}{G'} \exp(-G) \Big|_{\delta_{\text{eff}}=\delta_c(z_c)}. \quad (57)$$

Note that the remaining $1/2$ term on the r.h.s. of equation (56) has been exactly canceled by the pole residual of the integral at $G'(\delta_{\text{eff}}) = 0$. The latter formula provides an accurate approximation of the level-crossing probability $P(> \delta_c)$, provided the cumulant generator $\mathcal{M}(\delta_{\text{eff}})$ is analytic for all finite values of its argument, which is indeed the case for our approximated expression in eq. (50), but certainly not for the exact form of eq. (27). The validity of our last result will then rely on the smallness of the non-Gaussianity parameter ϵ . It is important to notice here that since - as it is clear from Figure 1 - the skewness parameter is not small everywhere, we expect the PDF to be very sensitive to small ϵ at least for model A.

The approximate form of the effective action resulting from Legendre transforming eq. (50) is

$$G(\delta_{\text{eff}}) \approx \frac{\delta_{\text{eff}}^2}{2\sigma_R^2} \left\{ 1 - \epsilon^2 \left(6 \frac{\beta}{\alpha} \langle \phi^2 \rangle + \frac{\mu_{2,R}^{(2)}}{\sigma_R^2} \right) - \frac{S_{3,R}}{3} \delta_{\text{eff}} + \left[\frac{1}{4} S_{3,R}^2 - \frac{1}{12} \left(1 + \frac{1}{2} \alpha \beta \right) S_{4,R} \right] \delta_{\text{eff}}^2 \right\}. \quad (58)$$

The level crossing probability $P(> \delta_c)$ to second order in ϵ can be obtained from (57), with (57) and the following substitution:

$$\frac{(G'')^{1/2}}{G'} = \frac{\sigma_R}{\delta_{\text{eff}}} \left[1 + \frac{\epsilon^2}{24\alpha} \left(72\beta \langle \phi^2 \rangle \sigma_R^2 - \alpha^2 \beta \delta_{\text{eff}}^2 \sigma_R^2 S_4^{(2)} + 12\alpha \mu_2^{(2)} + 3S_3^{(1)} \alpha \delta_{\text{eff}}^2 \sigma_R^2 - 2\delta_{\text{eff}}^2 \sigma_R^2 \alpha S_4^{(2)} \right) \right] \quad (59)$$

To linear order in ϵ the effective action reads

$$G(\delta_{\text{eff}}) \approx \frac{\delta_{\text{eff}}^2}{2\sigma_R^2} \left\{ 1 - \frac{S_{3,R}}{3} \delta_{\text{eff}} \right\}. \quad (60)$$

Note that this function is only convex for $\delta_{\text{eff}} < 1/S_{3,R}^{(1)}$, so that our result can be consistently applied only as long as $\delta_c(z_c) < 1/S_{3,R}^{(1)}$.

We finally obtain

$$P(> \delta_c | z_c, R) \approx \frac{1}{\sqrt{2\pi}} \frac{\sigma_R}{\delta_c(z_c)} \exp \left[-\frac{1}{2} \frac{\delta_c^2(z_c)}{\sigma_R^2} \left(1 - \frac{S_{3,R}}{3} \delta_c(z_c) \right) \right]. \quad (61)$$

Note that, for the Gaussian case, $S_{3,R} = 0$, this formula corresponds to the well-known asymptotic behaviour of the complementary error function valid where $\delta_c \gg 2\sigma$. In particular, for $S_{3,R} = 0$, and $z = 0$ this approximation introduces an error of 20% at $R \sim 10 \text{ Mpc } h^{-1}$ and an error smaller than 5% for $R > 20 \text{ } h^{-1} \text{ Mpc}$.

For $\delta_c(z_c) \geq 1/S_{3,R}$, i.e. for $R \lesssim 10 \text{ Mpc}$ and/or $\epsilon \gtrsim 10^{-3}$ for model A, the integral (54) has to be performed numerically. To first order in ϵ eq. (54) becomes:

$$P(> \delta_c | z_c, R) = \frac{1}{2} - \frac{1}{\pi} \int_0^\infty \frac{d\lambda}{\lambda} \exp(-\lambda^2 \sigma_R^2 / 2) \sin(\lambda \delta_c + \lambda^3 \mu_{3,R} / 6). \quad (62)$$

In Figure 4 we show the result of the numerical integration for model A for masses in the range $10^8 - 10^{12} M_\odot$, redshift $z_c = 6, 8, 10$ and ϵ from top to bottom $\epsilon = 10^{-2}, 5 \times 10^{-3}, 2 \times 10^{-3}, 10^{-3}, 5 \times 10^{-4}$, and the Gaussian case ($\epsilon = 0$, solid line). The main effect of the presence of a small non-Gaussianity such as $\epsilon = 5 \times 10^{-4}$, is to amplify $P(> \delta_c | z_c, R)$ by a factor of order 10.

For model B instead, as shown in Figure 2, the skewness parameter for the density field is small and has the opposite sign of ϵ . For this reason the saddle-point approximation (60) works remarkably well on galaxy scales for $|\epsilon| \lesssim 500$, if $z_c \lesssim 10$. Figure 5 shows the excursion set probability for model B for masses in the range $10^8 - 10^{12} M_\odot$, redshift $z_c = 6, 8, 10$ and ϵ from top to bottom $\epsilon = -300, -200, -100, 0, 100, 200$. The thick solid line is relative to the Gaussian case ($\epsilon = 0$); curves above that have $\epsilon < 0$, below have $\epsilon > 0$. The fact that $|\epsilon| \sim 100$ is needed to create any sizeable departure from the Gaussian $P(> \delta_c | M)$, has an important consequence: all conventional inflationary models induce deviations from Gaussianity such that the skewness parameter for the peculiar gravitational potential $S_{3,\Phi}$ is bound to be $|S_{3,\Phi}| \lesssim 10$ (Gangui et al. 1994); since $S_{3,\Phi} \sim 6\epsilon$, we conclude that, in the context of single-field inflation models the level-crossing probability $P(> \delta_c | M)$ is indistinguishable from the Gaussian one at least on clusters scale and below. It is important to stress that for this model, using values of ϵ of order unity or even larger does not imply the breakdown of the perturbation expansion upon which our results rely, as the coefficients of that expansion, such as the skewness parameter, keep small even for $|\epsilon| \lesssim 100$.

The most complex issue is that of finding a suitable expression for the function $P(M|M')$ in equation (51) in the general non-Gaussian case and for generic filters. In this context, it is useful to define a ‘fudge factor’ f through the equation

$$P(M|M') \equiv \frac{1}{f} \Theta(M' - M), \quad (63)$$

with Θ the Heaviside step function. As shown by Nagashima & Gouda (1997), in the Gaussian case, with sharp-k-space filtering, $P(M|M')$ reduces to the conditional probability $P(\delta_M \geq \delta_c | \delta_{M'} = \delta_c)$, which is easily obtained from a bivariate Gaussian, using Bayes theorem; from this one immediately gets $f = 2$, as expected (e.g. Peacock & Heavens 1990). In the non-Gaussian case (and/or for different types of filter) the value of f should be obtained from its very definition. Recently, Koyama, Soda & Taruya (1999) showed that in generic non-Gaussian models one can still write

$$f(M, M') \approx \left[\int_{\delta_c} d\omega p(\delta_M = \omega | \delta_{M'} = \delta_c) \right]^{-1}, \quad (64)$$

with $p(\delta_M = \omega | \delta_{M'} = \delta_c) \approx p(\delta_M = \omega - \delta_c)$, provided $M' \gg M$. Obtaining a similar relation for *all* scales $M' > M$ is a more complex issue, which would require a separate analysis⁸. Nonetheless, it is extremely reasonable to expect that this approximation works well at least in so far as the deviation from Gaussianity is weak. One then immediately gets the simple result⁹ $f \approx 1/P(> 0|M)$. In our case, one can compute the cumulative zero-crossing probability $P(> 0, M)$ numerically, starting from eq. (62).

The comoving mass-function of halos formed at redshift z_c can thus be immediately obtained by differentiating the integral equation (51). This allows the standard PS formula to be extended to the non-Gaussian case in the simple form (Lucchin & Matarrese 1988; Colafrancesco et al. 1989; Chiu et al. 1998; Robinson et al. 1999a,b; Koyama et al. 1999):

$$n(M, z_c) = f \frac{3H_0^2 \Omega_{0m}}{8\pi GM} \left| \frac{dP(> \delta_c | z_c, R)}{dM} \right|, \quad (65)$$

where we implicitly assumed that the value of f has negligible dependence on M . The factor f should account for the physical constraint that all of the clustered matter in the Universe must be included in bound objects of some mass [i.e. $\int_0^\infty dM M n(M, z_c) = 3H_0^2 \Omega_{0m} / 8\pi G$] and simultaneously solve the cloud-in-cloud problem.

For the non-Gaussian models considered here, the factor f is not much different from the Gaussian value, provided ϵ is small, i.e. for small departures from the Gaussian behaviour. In Figure 8 the fudge factor $f \simeq 1/P(> 0|M)$ is plotted as a function of the skewness parameter, using a top-hat filter in real space. The useful range is on the left of the vertical dotted line, that is $M \gtrsim 2 \times 10^{10} M_\odot$ for model A with $\epsilon = 10^{-3}$ and $M \lesssim 4 \times 10^{15} M_\odot$ for model B with $\epsilon = -100$. We can therefore conclude that, for mild non-Gaussianity, the correction to the usual fudge factor $f = 2$ is negligible when compared to the effect of the skewness term in the exponential, justifying therefore the use of $f = 2$ throughout.

4.1. Model A

In model A the skewness parameter $S_{3,R}$ is scale-independent on large scales, therefore, as a first step, we can neglect the dependence of $S_{3,R}$ on mass. In this case, in the above differentiation, we arrive to a very simple generalization of the PS formula, which has the same functional form,

⁸In the Gaussian case, and for sharp-k-space filter, one finds $p(\delta_M = \omega | \delta_{M'} = \delta_c) = p(\delta_{\tilde{M}} = \omega - \delta_c)$, for all $M' > M$, where \tilde{M} is defined by $\sigma^2(\tilde{M}) = \sigma^2(M) - \sigma^2(M')$. Inserting this result in eq. (64) yields $f = 2$, independently of the mass (Nagashima & Gouda 1997).

⁹Note that, if the non-Gaussian PDF depends on the filtering mass only through the variance, i.e. $P(\delta_M) = \sigma_M^{-1} \Psi(\delta_M / \sigma_M)$, as assumed by Willick (1999), then $P(> 0|M) = P(> \delta_c | M = 0)$, which yields an alternative expression for f , used by some authors (e.g. Robinson & Baker 1999). In the most general case, however, the latter result is not valid.

provided one makes the replacement

$$\delta_c(z_c) \rightarrow \delta_c(z_c) \left[1 - \frac{S_{3,R}}{3} \delta_c(z_c) \right]^{1/2} \equiv \delta_*(z_c) \quad (66)$$

and therefore:

$$n(M, z_c) \simeq f \frac{3H_0^2 \Omega_{0m}}{8\pi G M^2} \frac{\delta_*(z_c)}{\sqrt{2\pi} \sigma_M} \exp \left[-\frac{\delta_*^2(z_c)}{2\sigma_M^2} \right] \left| \frac{d \ln \sigma_M}{d \ln M} \right| \quad (67)$$

This simple result is completely analogous to that found by Lucchin & Matarrese (1988), for hierarchical-type statistics: the effect of the deviation from primordial Gaussianity is that of shifting the PS characteristic mass to higher or lower masses, depending on whether the skewness is positive or negative. Note that the effect of the non-Gaussian tail becomes more and more important at higher redshifts. As noticed by Fry (1986), ‘the departures from Gaussian can be appreciable while fluctuations are still small’. The assumption that $S_{3,R}$ is scale-independent is correct on relatively large scales, where $R > 20 h^{-1}$ Mpc, corresponding to masses $M > 10^{14} M_\odot$. Substitution (66) applied to the standard PS formalism agrees with the numerical results on scales $R > 20 h^{-1}$ Mpc, for $\epsilon \lesssim 10^{-2}$. The dependence on the cosmological model is confined to $\delta_c(z_c)$, as discussed before, once the present-day power-spectrum shape and normalization have been chosen, and the normalization $H_0^2 \Omega_{0m}$.

However from Figure 1 it is clear that the scale dependence of $S_{3,R}^{(1)}$ is not negligible for galaxy masses, moreover for $R \lesssim 10$ i.e. $M \lesssim 10^{13}$ the saddle-point approximation does not hold. Numerical evaluation of (54) yields $dP(> \delta_c)/dM$; the corresponding $n(M, z_c)$ is shown in Figure 6 for the same range of masses, redshift of collapse z_c and non-Gaussianity parameter ϵ as in Figure 4, assuming $f = 2$, according to the discussion above.

4.2. Model B

It is clear from the scale dependence of the skewness parameter that, for departures from Gaussianity of the kind of model B, clusters scales are better than galaxy scales to probe primordial non-Gaussianity. It is worth to notice here that also for model B in the absence of the transfer function, $S_{3,R}$ is scale independent and indeed the skewness parameter becomes scale-independent on very large scales ($R \gtrsim 100 h^{-1}$ Mpc), where the transfer function is unity. On clusters scales $S_{3,R}$ is not scale-independent, but for $\epsilon \lesssim 200$ and redshift $z_c \lesssim 2$ the saddle-point approximation is still valid. For the comoving mass-function of halos formed at redshift z_c we obtain:

$$n(M, z_c) \simeq f \frac{3H_0^2 \Omega_{0m}}{8\pi G M^2} \frac{1}{\sqrt{2\pi} \sigma_M} \left| \frac{1}{2} \frac{\delta_c^2(z_c)}{3\sqrt{1 - S_{3,M} \delta_c(z_c)/3}} \frac{dS_{3,M}}{d \ln M} + \frac{\delta_*(z_c)}{\sigma_M} \frac{d \ln \sigma_M}{d \ln M} \right| \exp \left[-\frac{\delta_*^2(z_c)}{2\sigma_M^2} \right] \quad (68)$$

Also in this case the dependence on the cosmological model is confined to $\delta_c(z_c)$ and in the normalization $H_0^2 \Omega_{0m}$. Figure 7 illustrates the effect on the mass-function on clusters scales for the non-Gaussianity of model B. For two different redshifts of collapse ($z_c = 1$ and 2) the ratio of

the mass-function for model B to the mass-function for a Gaussian field [$n(M, z_c)/n_{\text{Gau}}(M, z_c)$] is plotted as a function of the mass in solar masses. Also in this case we can assume $f = 2$. The choice for the ϵ parameter is, from top to bottom, $\epsilon = -100, -50, -10$. It is clear that for high masses one is probing the tail of the distribution, that is most sensitive to departures from Gaussianity. The forthcoming X-ray Multi-Mirror (XMM) galaxy cluster survey (Romer et al. 1999), will allow the number density of clusters to be accurately measured even at $z \gtrsim 1$. In particular the XMM cluster survey will provide a complete survey of clusters with masses $M \gtrsim 10^{14} M_{\odot}$ at $z < 1.4$ over 800 square degrees. Preliminary calculations suggest that it will be therefore possible to detect $|\epsilon| \gtrsim 50$.

5. A worked example: galaxies at $z > 5$

The technique presented in the previous section allows one to measure *accurately* the amount of non-Gaussianity on a given scale. Although the traditional route has been to use the abundance of clusters, we will illustrate our technique by using the observed abundance of high- z galaxies (e.g. Cavaliere & Szalay 1986; Kashlinsky & Jimenez 1997; Peacock et al. 1998). There are some advantages in using high- z galaxies: they sample directly the galaxy scale and the objects are always inside virialised halos. One major disadvantage is that the mass is not accurately determined. On the other hand, as larger telescopes, such as NGST, get on line, it will be possible to obtain volume limited samples of high- z galaxies and from high-resolution spectra, dynamical masses will be determined more accurately. As seen from eq. (66), it is clear that the higher the redshift the more sensitive the PDF is to non-Gaussianity. Up to date there are 6 galaxies with spectroscopic redshifts observed between $z > 5$ to $z \approx 7$ (Dey et al. 1998; Spinrad et al. 1998; Weymann et al. 1998; Hu et al. 1999; Chen et al. 1999) and in Table 1 we have compiled their most relevant characteristics. These high- z galaxies have been found in relatively small areas of the sky: for the purposes of this worked example we will use a scanned area of 3×10^{-4} square degrees for each galaxy ¹⁰.

As pointed out before, the masses of this high- z sample are unknown, but their *current obscured* star formation rate is known. The first step is to correct the observed star formation rate for the presence of dust. In (Jimenez et al. 1999) a case has been made for the correction factor for the star formation due to the presence of dust in a starburst being ~ 5 (independently of the magnitude of the host galaxy). This is confirmed by the independent arguments presented in Peacock et al. (1999). The corrected star formation rate is presented in Table 1. Since the age of the Universe at $z \approx 6$ is already about 0.7 Gyr even for EdS, assuming the present age to be 13 Gyr, it is very unlikely that galaxies have been observed just when their stellar populations are born. Note

¹⁰Four of the six galaxies considered here have been found in the Hubble Deep field, where the total area scanned is about $\sim 1/800$ of a square degree. The other two galaxies have been found in Keck observations, where the area scanned for each of them is about 7.4×10^{-5} square degrees. For this worked example we will therefore make the conservative choice that there is on average one galaxy per 3×10^{-4} square degrees.

that galaxies are likely to be dust–enshrouded for about 0.02 Gyr (Jimenez et al. 1999) and thus be invisible for about 3% of the Hubble time at $z \approx 6$. The star formation rate of the galaxy in the past is more likely to be higher (Heavens & Jimenez 1999) than the present observed one. To account for this we will then assume that the galaxy has been observed when it is 0.1 Gyr old (i.e. about 10% of the Hubble time at $z \approx 6$) and has been forming stars at the current (constant) observed rate. Using this, we can estimate what the mass in stars in the galaxies (see Table 1) and in dark matter is, using a simple isothermal profile for the halo, i.e. $M = V_c^3/(10GH(z_c))$, where z_c is the redshift of collapse¹¹ and assuming that $\Omega_{ob} = 0.015h^{-2}$. Following Peacock et al. (1998) we will carry out our analysis in terms of σ_v . For an isothermal halo $\sigma_v = V_c/\sqrt{2}$. Table 1 shows that $\sigma_v = 70 - 200 \text{ km s}^{-1}$. The number density of high- z galaxies is $N(\Omega = 1) \gtrsim 3.6 \times 10^{-3}(h^{-1}\text{Mpc})^{-3}$ [$N(\Omega_0 = 0.3, \Lambda_0 = 0.7) \gtrsim 8.3 \times 10^{-4}(h^{-1}\text{Mpc})^{-3}$].

To compare these observations with our theoretical results we integrate the mass-function to obtain the number of galaxies observed per unit volume with redshift of formation $6 < z_c < 8$ and masses $2 \times 10^{10}M_\odot < M < 4 \times 10^{11}M_\odot$. It is worth noting that our mass estimates slightly underpredict the masses that are derived using the width of the $Ly\alpha$ line (Dey et al. 1998). Gaussian initial conditions give $N(\Omega_0 = 0.3, \Lambda_0 = 0.7) = 5.2 \times 10^{-5}(h^{-1}\text{Mpc})^{-3}$, which is about a factor sixteen lower than the observed value. For Model A with $\epsilon = 10^{-3}$, we obtain $N(\Omega_0 = 0.3, \Lambda_0 = 0.7) = 1.3 \times 10^{-3}(h^{-1}\text{Mpc})^{-3}$, which is much closer to the observed value. As we already noted before, a very small non-Gaussianity parameter (i.e. a very small departure from the Gaussian behaviour) has a dramatic effect on the statistics of high redshift objects. This is, of course, very preliminary. For the tail of the PDF, the mass function is very sensitive to the overdensity threshold, the mass determination and the redshift of formation. In this example we have assumed that the redshift of formation is the redshift at which the object has been observed. This is of course quite a conservative assumption, yielding a lower limit on the non-Gaussianity parameter. It has been shown that the PS algorithm with a fixed threshold δ_c does not reproduce very accurately N-body simulation results (e.g. Sheth & Tormen 1999). However, the deviations on the mass scales considered here are never larger than a factor of a few, well below the uncertainty due to the mass determination (see below). PS predictions and N-body results can be reconciled by making the threshold for collapse scale-dependent (e.g. Sheth & Tormen 1999; Sheth, Mo & Tormen 1999). This will change the absolute prediction on the number density of objects but will not strongly affect the ratio between the Gaussian and non-Gaussian number density predictions. The spherical collapse assumption underlying the PS algorithm is the main reason why theory does not reproduce accurately N-body results: the introduction of the ellipsoidal collapse improve sensibly the agreement (Lee & Shandarin 1998). In a subsequent paper we will address the issue of triaxial collapse for non-Gaussian initial conditions.

¹¹Although we have assumed that the stellar population of the galaxy has to be about 10% of the Hubble time at the observed redshift, we will conservatively consider that the dark halo has just collapsed at the observed redshift. This is what is expected in hierarchical models, where the stellar population is generally made in previous generations inside smaller haloes.

Maybe the most pressing issue is that of the mass determination of high-redshift objects. For example, if the mass estimate for the galaxies in the worked example is wrong by a factor of 4, the number density would change by a factor of 20 (at $z_c = 6$), and agreement between predictions and observations could be obtained without resorting to $\epsilon \neq 0$.

Indeed, better observations will improve the determination of the mass of the dark halos and of the number density of high redshift galaxies. A measurement of ϵ and thus a determination of the amount of primordial non-Gaussianity (if any!) present on galaxy scales will then become possible.

6. Conclusions

We have shown that it is possible to test whether initial conditions were Gaussian, by looking at the abundance of galaxies and clusters at high redshift. Small deviation from Gaussianity have a deep impact on those statistics which probe the tail of the distribution: for this reason the abundance of high redshift objects such as galaxies at $z \gtrsim 5$ and clusters at $z \gtrsim 1$, is very sensitive to small departures from the Gaussian behaviour.

We used a parameterization of primordial non-Gaussianity that covers a wide range of physically motivated models: the non-Gaussian field is given by a Gaussian field plus a term proportional to the square of a Gaussian field, the proportionality constant being the non-Gaussianity parameter. We applied this model to the primordial density fluctuation field and to the gravitational potential fluctuation field, and we assumed that the departures from the Gaussian behaviour are small. Given this parameterization of non-Gaussianity, we were able to obtain an analytic expression for the probability density function (PDF) of the smoothed density field. This approach is somewhat different from what is found in the literature (e.g. Robinson et al. 1999a,b), since we do not assume a particular form for the non-Gaussian PDF, but we *derive* it, given a parameterization of the primordial non-Gaussianity.

We then introduced a generalized version of the PS approach valid in the context of non-Gaussian initial conditions, also tackling the cloud-in-cloud problem. This enabled us to relate, analytically, the non-Gaussianity parameter to the number of high-redshift objects. The strength of our method is that we are able to properly take into account the smoothing scale, or mass, dependence of the probability distribution function, and that our results are analytic. In looking at the likelihood of rare events for a non-Gaussian density field, one is probing the tail of the distribution, and analytical results are not only elegant but also extremely important.

The main technical results of the present paper can be summarized as follows: a) Eq. (27) is the exact analytic form of the cumulant generator for our non-Gaussian models: it can be used to generate cumulants of any order by simple differentiation. b) Eq. (54): this equation gives an exact and general analytic expression for the cumulative probability that, at a given redshift z_c , the fluctuations on scale R exceed some critical value δ_c . From this expression it is possible to obtain

the cumulative probability to any order by expanding the cumulant generator (36) with (40) and (41) as we did in (50). c) Eq. (61): it is an analytic expression for the cumulative probability valid for small deviations from the Gaussian behaviour. d) Eq. (68), with the definition (66): it is an analytic expression for the comoving mass-function of halos obtained within the PS approach. For a given power spectrum the dependence on the cosmological model is straightforward: it is confined to the normalization factor $H_0^2 \Omega_{0m}$ and the threshold δ_c .

Still an important issue remains unsolved: how to accurately determine the mass and the formation redshift of observed high-redshift objects in order to put tight constraints on primordial non-Gaussianity. This issue will be addressed in a forthcoming paper.

LV acknowledges the support of a TMR grant. LV and RJ thank A. Berera, A. Heavens and J. Peacock for stimulating discussions and the anonymous referee for useful comments. SM thanks K. Jedamzik, H. J. Mo and R. Sheth for useful discussions.

REFERENCES

- Albrecht, A. & Stebbins, A. 1992, *Phys. Rev. Lett.*, 68, 2121
- Allen, T. J., Grinstein, B., & Wise, M. B. 1987, *Phys. Lett. B*, 197, 66
- Avelino, P. P. & Viana, P. 1999, preprint, astro-ph/9907209
- Bardeen, J. M., Bond, J. R., Kaiser, N., & Szalay, A. S. 1986, *ApJ*, 304, 15
- Bertschinger, E. 1987, *ApJ(Lett)*, 323, 103
- Bond, J. R., Cole, S., Efstathiou, G., & Kaiser, N. 1991, *ApJ*, 379, 440
- Bouchet, F. R. & Gispert, R. 1999, *New Astronomy*, astro-ph/9903176
- Cavaliere, A. & Szalay, A. 1986, *ApJ*, 311, 589
- Chen, H. W., Lanzetta, K. M., & Pascarella, S. 1999, *Nature*, 398, 586
- Chiu, W. A., Ostriker, J., & Strauss, M. A. 1998, *ApJ*, 494, 479
- Colafrancesco, S., Lucchin, F., & Matarrese, S. 1989, *ApJ*, 345, 3
- Cole, S. 1991, *ApJ*, 367, 45
- Coles, P., Barrow, J. D. 1987, *MNRAS*, 228, 407
- Cornwall, J. M., Jackiw, R., & Tomboulis, E. 1974, *Phys. Rev. D*, 10, 2428
- Dey, A., Spinrad, H., Stern, D., Graham, J. R., & Chaffee, F. H. 1998, *ApJ(Lett)*, 498, L93

- Eke, V. R., Cole, S., & Frenk, C. S. 1996, MNRAS, 282, 263
- Falk, T., Rangarajan, R., & Srednicki, M. 1993, ApJ(Lett), 403, 1
- Fan, Z. & Bardeen, J. M. 1992, University of Washington preprint
- Fry, J. N. 1985, ApJ, 289, 10
- 1986, ApJ(Lett), 308, 71
- Gangui, A. 1994, Phys. Rev. D, 50, 3684
- Gangui, A., Lucchin, F., Matarrese, S., & Mollerach, S. 1994, ApJ, 430, 447
- Gangui, A. & Martin, J. 1999, astro-ph/9908009
- Grinstein, B. & Wise, M. B. 1986, ApJ, 310, 19
- Gunn, J. & Gott, R. 1972, ApJ, 176, 1
- Hawking, S. & Moss, I. G. 1983, Nuclear Physics B, 224, 180
- Heavens, A. F. & Jimenez, R. 1999, MNRAS, 305, 770
- Hill, C. T., Schramm, D. N., & Fry, J. N. 1989, Comments Nucl. Part. Phys., 19, 25
- Hu, W., Spergel, D. N., & White, M. 1997, Phys. Rev. D, 55, 3288
- Hu, E. M., McMahon, R. G., & Cowie, L. L. 1999, ApJ(Lett), 522, L9
- Jedamzik, K., 1995, ApJ, 448, 1
- Jimenez, R., Padoan, P., Dunlop, J. S., Bowen, D., Juvela, M., Matteucci, F. 1999, ApJ in press, astro-ph/9910279
- Kashlinsky, A. & Jimenez, R. 1997, ApJ, 474, L81
- Kitayama, T. & Suto, Y. 1996, ApJ, 469, 480
- Knox, L. 1999, MNRAS, 307, 977
- Kofman, L. & Pogosyan, D. Y. 1988, Phy. Rev. Lett. B, 214, 508
- Koyama, K., Soda, J., & Taruya, A. 1999, MNRAS, in press, astro-ph/9903027
- Lacey, C. & Cole, S. 1993, MNRAS, 262, 627
- Lee, J. & Shandarin, S. F. 1998, ApJ, 500, 14
- Linde, A. D. & Mukhanov, V. 1997, Phys. Rev. D, 56, 535

- Lucchin, F. & Matarrese, S. 1988, *ApJ*, 330, 535
- Luo, X. 1994, *ApJ(Lett)*, 427, 71
- Matarrese, S., Lucchin, F. & Bonometto, S. 1986, *ApJ(Lett)*, 310, 21
- Moscardini, L., Matarrese, S., Lucchin, F., & Messina, A. 1991, *MNRAS*, 248, 424
- Nagashima, M., Gouda, N. 1997, *MNRAS*, 287, 515
- Peacock, J. A. & Heavens, A. F. 1990, *MNRAS*, 243, 133
- Peacock, J. A., Jimenez, R., Dunlop, J. S., Waddington, I., Spinrad, H., Stern, D., Dey, A., & Windhorst, R. A. 1998, *MNRAS*, 296, 1089
- Peacock et al. 1999, *MNRAS*, astro-ph/9912231
- Peebles, P. J. E 1980, *The Large-Scale Structure of the Universe*, Princeton University Press.
- 1999a, *ApJ*, 510, 523
- 1999b, *ApJ*, 510, 531
- Pen, U.-L. & Spergel, D. N. 1995, *Phys. Rev. D*, 51, 4099
- Politzer, H. D. & Wise, M. B. 1984, *ApJ(Lett)*, 285, 1
- Press, W. H. & Schechter, P. 1974, *ApJ*, 187, 425
- Ramond, P. 1989, *Field Theory: a Modern Primer* (Frontiers in Physics Series, Vol 74)
- Robinson, J. & Baker, J. 1999, *ApJ*, astro-ph/9905098
- Robinson, J., Gawiser, E., & Silk, J. 1999a, *ApJ(Lett)*, astro-ph/9805181
- 1999b, *ApJ*, submitted, astro-ph/9906156
- Romer, K. A., Viana, P. T. P., Liddle A. R., & Mann, R. G. 1999, astro-ph/9911499
- Salopek, D. 1999, astro-ph/9903327
- Salopek, D., Bond, J. R., & Bardeen, J. M. 1989, *Phys. Rev. D*, 40, 1753
- Spinrad, H., Stern, D., Bunker, A., Dey, A., Lanzetta, K., Yahil, A., Pascarelle, S., & Fernandez-Soto, A. 1998, *AJ*, 116, 2617
- Sugiyama, N. 1995, *ApJ Suppl.*, 100, 281
- Taylor, A. N. & Watts, P. R. 2000, *MNRAS*, in press, astro-ph/0001118

- Tegmark, M. 1998, *ApJ*, 502, 1
- Tegmark, M. 1996, *ApJ Lett*, 464, 35
- Turok, N. 1989, *Phys. Rev. Lett.*, 63, 2625
- Vachaspati, T. 1986, *Phys. Rev. Lett.*, 57, 1655
- Verde, L., Wang, L., Heavens, A. F., & Kamionkowski, M. 1999, *MNRAS*, astro-ph/9906301
- Viana, P. & Liddle, A. 1998, *MNRAS*, 303, 535
- Vilenkin, A. 1985, *Phys. Rep.*, 121, 263
- Wang, L. & Kamionkowski, M. 1999, *Phys. Rev. D* submitted, astro-ph/9907431
- Wang, Y., Spergel, D. N., & Strauss, M. A. 1999, *ApJ*, 510, 20
- Weymann, R. J., Stern, D., Bunker, A., Spinrad, H., Chaffee, F. H., Thompson, R. I., & Storrie-Lombardi, L. J. 1998, *ApJ(Lett)*, 505, L95
- White, S. D. M., Efstathiou, G., & Frenk, C. 1993, *MNRAS*, 262, 1023
- Willick, J. A. 1999, *ApJ*, submitted, astro-ph/9904367
- Yano, T., Nagashima, M., & Gouda, N., 1996, *ApJ*, 466, 1
- Zel'dovich, Ya. B., Molchanov, S. A., Ruzmaikin, A. A., & Sokolov, D. D. 1987, *Sov. Phys. Usp.*, 30, 5

Figure 1: Model A variance, skewness ($\mu_{3,R}^{(1)}$) and skewness parameter ($S_{3,R}^{(1)}$) as a function of the radius of the top-hat window in real space and of the mass. To produce this plot we assumed: $\alpha = 1$, a scale-invariant initial power-spectrum $P_\phi \propto k$, CDM transfer function, $\Omega_{0m} = 0.3$, normalized to produce $\sigma_8(z = 0) = 1$ (more details in the text).

Figure 2: Model B variance, skewness ($\mu_{3,R}^{(1)}$) and skewness parameter ($S_{3,R}^{(1)}$) as a function of the radius of the top-hat window in real space and of the mass. To produce this plot we made the same assumptions as for Figure 1 except that now $P_\phi \propto k^{-3}$.

Figure 3: Left panel: The redshift dependence of the threshold for collapse Δ_c in different cosmologies. It is clear that the dependence on redshift and on cosmology is weak. This justifies to assume $\Delta_c = 1.687$ throughout. Middle panel: Dependence of the relation between dark mass and radius on the cosmology and the redshift of collapse z_c . The solid lines denote an Einstein de Sitter Universe, the dashed lines a flat model with $\Omega_{0m} = 0.3$ and $\Lambda_0 = 0.7$ and the dotted lines an open model with $\Omega_{0m} = 0.3$. The dependence is very weak and can be safely ignored. Right panel: The redshift dependence of the inverse of the linear fluctuation growth for different cosmologies.

Figure 4: Model A $P(> \delta_c | z_c, R)$ for $z_c = 6$ (left panel), $z_c = 8$ (center), $z_c = 10$ (right panel) and $\epsilon = 10^{-2}, 5 \times 10^{-3}, 2 \times 10^{-3}, 10^{-3}, 5 \times 10^{-4}$. The thick solid line is relative to the Gaussian case. It is clear that the main effect of the presence of a small nonzero ϵ is to boost $P(> \delta_c | z_c, R)$ by at least a factor ~ 10 .

Figure 5: Model B $P(> \delta_c | z_c, R)$ for $z_c = 6$ (left panel), $z_c = 8$ (center), $z_c = 10$ (right panel) and $\epsilon = -300, -200, -100, 0, 100, 300$ (from top to bottom). The thick solid line is relative to the Gaussian case. It is clear that $|\epsilon_B|$ of model B need to be $\gg \epsilon_A$ of model A to show a noticeable difference from the Gaussian case. Moreover $\epsilon_B < 0$ is needed in order to enhance the non-Gaussian tail of $P(> \delta_c | z_c, R)$.

Figure 6: Model A: The comoving mass-function of halos formed at redshift 6 (left panel) 8 (center), 10 (right panel), for different values of the non-Gaussian parameter ϵ , as in Figure 4; from top to bottom: $\epsilon = 10^{-2}, 5 \times 10^{-3}, 2 \times 10^{-3}, 10^{-3}, 5 \times 10^{-4}$. The thick solid line is relative to the Gaussian case.

Figure 7: Model B: The non-Gaussian effect on the mass-function on clusters scales. For two different redshift of collapse ($z_c = 1$ left and $z_c = 2$ right) the ratio of the mass-function for **model B** to the mass-function for a Gaussian field [$n(M, z_c)/n_{\text{Gau}}(M, z_c)$] is plotted as a function of mass. The choice for the ϵ parameter is, from top to bottom, $\epsilon = -100, -50, -10$. It is clear that for high masses one is probing the tail of the distribution, that is most sensitive to departures from Gaussianity.

Figure 8: The fudge factor $f \simeq 1/P(> 0|M)$ as a function of the skewness parameter. The value $f = 2$ is exact for the Gaussian case with sharp-k-space filter; the solid line shows the value of f as a function of the skewness parameter $S_{3,R}$. The useful range is on the left of the vertical dotted line, i.e. $M \gtrsim 2 \times 10^{10} M_\odot$ for model A with $\epsilon = 10^{-3}$ and $M \lesssim 4 \times 10^{15} M_\odot$ for model B with

$\epsilon = -100$. We can conclude that, for mild non-Gaussianity, the correction to the usual fudge factor is negligible, justifying therefore the use of $f = 2$ throughout.

Table 1: Main properties of observed galaxies at $z > 5$. Column 1: [1] Dey et al (1998); [2] Spinrad et al. (1998); [3] Weymann et al. (1998); [4] Hu, McMahon & Cowie (1999); [5] Chen, Lanzetta & Pascarella (1999). Column 2: spectroscopic redshift of the galaxy. Column 3: area of the sky (in square degrees) surveyed per galaxy. Column 4: observed star formation rate in solar masses per year (assuming $h = 0.65$). Column 5: dust corrected star formation rate (see text). Columns 6, 7: estimated mass in stars and dark matter (see text). Column 8: velocity dispersion obtained assuming an isothermal halo (see text).

Ref.	z	deg ²	$\frac{\text{obs.SFR}}{(M_{\odot}\text{yr}^{-1})}$	$\frac{\text{corr.SFR}}{(M_{\odot}\text{yr}^{-1})}$	$\frac{\text{est.}M_{*}}{M_{\odot}}$	$\frac{\text{est.}M_{\text{dark}}}{M_{\odot}}$	$\frac{\sigma_v}{(\text{kms}^{-1})}$
[1]	5.34	7.4×10^{-5}	4	20	2×10^9	2×10^{10}	70
[2]	5.34	3×10^{-4}	13	65	6.5×10^9	6.5×10^{10}	100
[2]	5.34	3×10^{-4}	13	65	6.5×10^9	6.5×10^{10}	100
[3]	5.60	3×10^{-4}	8	40	4×10^9	4×10^{10}	86
[4]	5.74	7.4×10^{-5}	40	200	4×10^{10}	4×10^{11}	187
[5]	6.68	3×10^{-4}	40	200	4×10^{10}	4×10^{11}	200

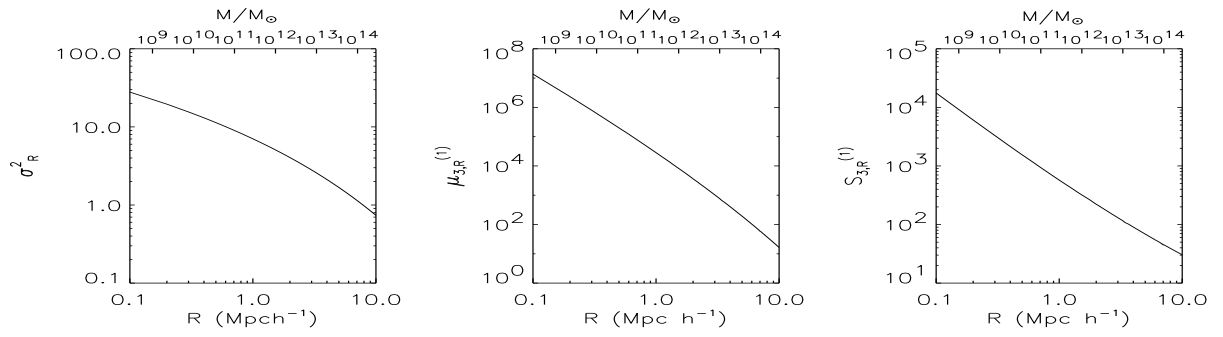


Fig. 1.—

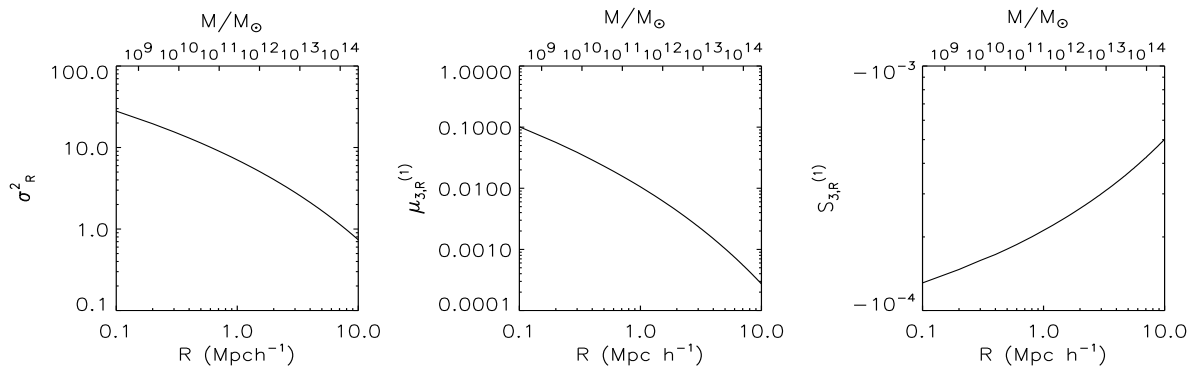


Fig. 2.—

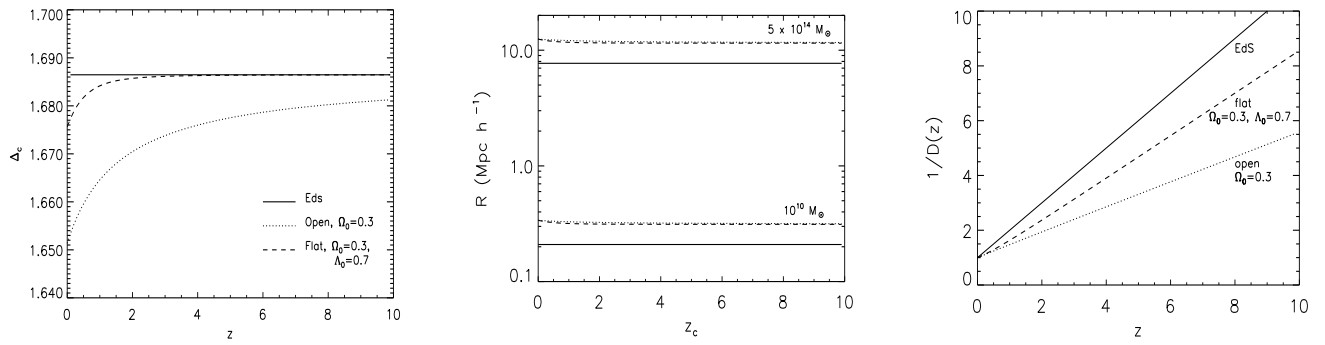


Fig. 3.—

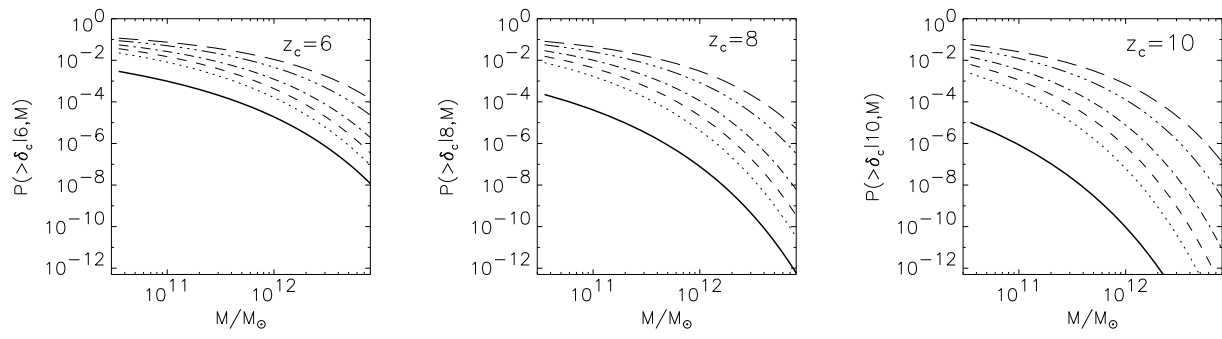


Fig. 4.—

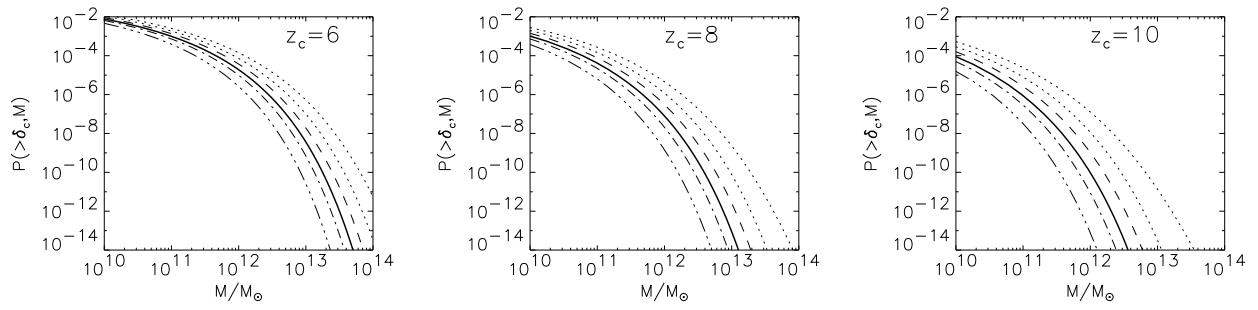


Fig. 5.—

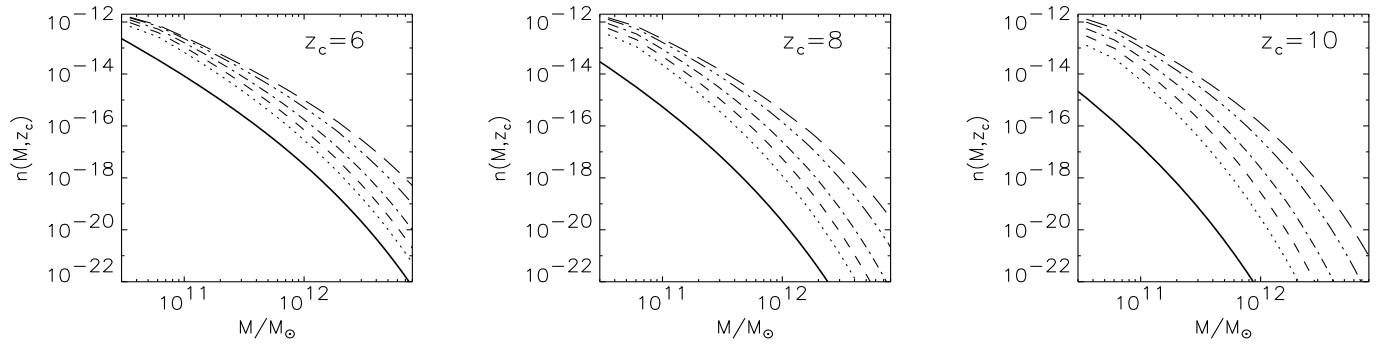


Fig. 6.—

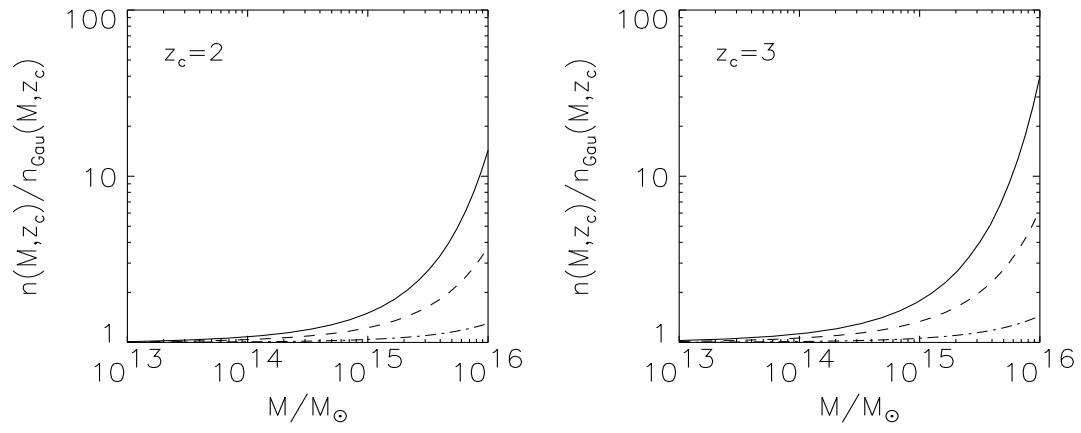


Fig. 7.—

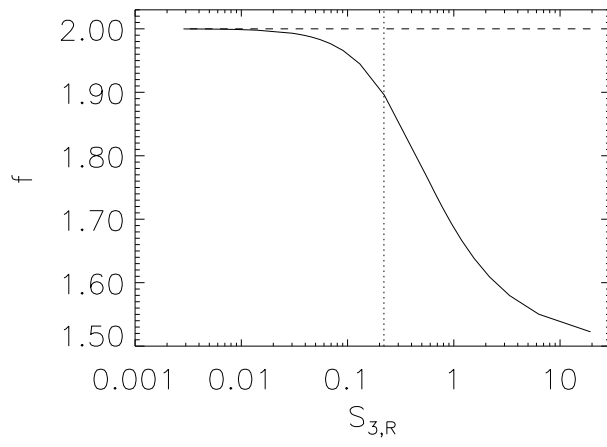


Fig. 8.—